Initial oxidation of ultrathin antimony films on Au(111) and of polycrystalline antimony

P. Ma and A. J. Slavin
Department of Physics, Trent University, Peterborough, Ontario, Canada K9J 7B8
(Received 13 September 1993)

It has been shown previously that antimony evaporated onto a Au(111) surface grows in a layer-by-layer mode. The present work compares the initial, fast-oxidation stage of these films with that on bulk polycrystalline antimony. Measurements were carried out in an ultrahigh-vacuum environment using Auger electron spectroscopy, low-energy electron diffraction, electron-energy-loss spectroscopy, and work-function change measurements. At 300 K and for oxygen pressures between 1×10^{-5} and 2×10^{-3} Torr, oxidation follows first-order Langmuir kinetics, with an initial sticking probability of about 10^{-5}. Oxidation essentially saturates by 10^{7} L (1 L $=10^{-6}$ Torr s). A layer of oxide about 8.5 Å thick is formed in this initial stage, both for Sb films and for bulk antimony. An initial antimony film on Au(111) of about 1.7 monolayers, or 1.6×10^{15} atoms/cm^2, is required to complete this oxide layer, for saturation oxidation. The chemical composition of the oxidized films and the oxidized surface of bulk antimony is Sb_2O_3. These results are compared with earlier work on Pb, Bi, and Sn.

I. INTRODUCTION

Oxidation of metals at room temperature and below, at least at low oxygen pressures, generally occurs in three stages: chemisorption, a fast-oxidation stage, and much slower field-assisted diffusion.[1,2] The first two stages are the ones which have been studied in most oxidation experiments in ultrahigh-vacuum (UHV) facilities near room temperature. It has been proposed[1] that the fast-oxidation stage occurs when a chemisorbed oxygen atom acquires electron charge from the metal; the force between this atom and its image charge is great enough to cause place exchange between the oxygen and a metal atom in the substrate. The oxide layer so produced can have a thickness of 1–4 atomic layers before the image force becomes too weak to break the metal-metal bond and cause place exchange. Earlier experiments in our laboratory indicate that this multilayer of oxide can grow on a bulk metal as a single structure which propagates across the metal surface. Formation of the multilayer requires a rearrangement of the near-surface substrate atoms, and it appears that it is favorable to rearrange the lower layer(s) at the same time as the outer one. This process will be aided by the heat of chemisorption.[1]

The present work extends previous studies on Pb,[3,4] Bi,[5] and Sn (Ref. 6) to include Sb. Pb and Bi are adjacent elements in the same row of the Periodic Table, with Sn and Bi lying just above them. The oxide growth on bulk polycrystalline Sb is compared with that on ultrathin films of Sb on a polished Au(111) surface. Since the Au does not oxidize in these experiments,[3] the Sb oxide can be built up a fraction of a monolayer at a time. This provides information about the oxidation process which cannot be obtained by oxidation of the bulk metal alone. In particular, it is possible to determine how much Sb is consumed in producing the oxide layer formed in the fast-oxidation stage. In addition, using an Sb layer which is thin enough to be fully oxidized provides an Sb Auger line shape from the oxide which can be used in the decomposition of Auger peaks on bulk Sb into oxidized and unoxidized components. This is not possible with oxidation of the bulk metal alone.

There have been relatively few experiments on the oxidation of Sb. Early work by Rosenberg, Butler, and Menna[7] inserted vacuum-crushed powders into a calibrated volume containing oxygen, and monitored the pressure decrease. Surface areas were determined using the Brunauer-Emmett-Teller (B.E.T.) equation. However, this work was not carried out under UHV conditions, and surface contamination was not monitored. More recently, Petit, Riga, and Caudano[8] measured oxide growth under UV laser irradiation, but concentrated their study on oxide growth after the fast-oxidation stage was complete. To our knowledge, ours is the first study of the fast-oxidation stage of Sb, under UHV conditions.

II. EXPERIMENT

It has been shown previously[9] that Sb deposited onto the Au(111) surface forms an Sb film which grows in a layer-by-layer fashion; each complete layer contains the same number of Sb atoms, and will be called a monolayer (ML). From this earlier work, the number of monolayers of Sb deposited can be determined from the ratio of the Auger amplitude of Sb to that of Au. Sb films up to 4.5 ML were used in the present experiment.

All measurements, using Auger electron spectroscopy (AES), low-energy electron diffraction (LEED), electron-energy-loss spectroscopy (EELS), and work-function measurements, have been carried out with a four-grid LEED system in an ultrahigh vacuum (UHV) chamber with a base pressure of 3×10^{-10} Torr, and with the sample at 300 K. We used the same gold sample and followed the same cleaning procedure as described elsewhere.[5] The oxide film was removed by argon bombardment at 830 K. The polycrystalline Sb (99.9999% pure, Johnson-Matthey) was mechanically cut and polished, and then cleaned by argon bombardment while heated at 600 K. The surfaces were monitored by AES before every experiment and no contamination was found. Sb

was deposited on Au(111) and the quantity determined as discussed above. Cold-trapped, ultrahigh-purity oxygen gas was used for oxidation of the Sb.

AES and EELS were recorded in the first derivative mode, although the EELS data are presented in the second derivative mode after spline smoothing of the raw data, so that the peaks occur at the loss energies. The intensity of the Auger signal was measured as the peak-to-peak height. The peaks used in the experiments were the following: Au ($N_{6,7}VV$, 69 eV), Sb ($M_4N_{4,5}N_{4,5}$, 457 eV), and O ($KL_{2,3}L_{2,3}$, 513 eV). For AES, the electron primary energy was 1500±0.2 eV, the beam current was 15.0±0.3 μA, and the peak-to-peak modulation voltages were 2.24, 8.49, and 11.0 V for the 69-, 457-, and 513-eV peaks, respectively. For the EELS spectra presented in this paper, the modulation voltage was 2.24 V (peak to peak), the primary energy was 100 eV, and the beam current 1.00 μA. For both AES and EELS, the primary beam current was measured as the current to the sample when the sample was held positive at 90 V. The onset method[10] was used to measure the work-function change with a 100-eV primary energy and 2.24-V (peak-to-peak) modulation. Sb does not oxidize easily: a 10^4-L (1 L$=10^{-6}$ Torr s) exposure was required for a measurable oxygen uptake. Therefore, relatively high oxygen pressures up to 2×10^{-3} Torr were used for oxidation.

Singh[11] has reported a measurable dissociation of the Sb_2O_3 surface to Sb after 15-min exposure to an electron beam of 2 keV, and 50 μA in a 0.25-mm-diameter spot. Since our primary beam current was only 15 μA for AES, and 1 μA for EELS, with a spot size of about 1-mm diameter and acquisition times of typically 5 min, dissociation should not have been a problem in these experiments. Indeed, no change in the Auger signals was seen for different acquisition times in our experiments.

III. RESULTS

A. AES on the bulk surface

Figure 1 shows the oxygen AES intensity as a function of the oxygen exposure at pressures ranging from 1×10^{-5} Torr at low exposures where adsorption was relatively rapid, to 2×10^{-3} Torr near saturation; in the inset, the exposure is plotted with a logarthmic scale to cover a wider range of exposures. For exposures less than 10^4 L, oxygen uptake was almost unobservable. The oxygen signal remained essentially constant after 10^7 L, even for an exposure of 10^{10} L. The data can be fitted well assuming first-order Langmuir kinetics, as shown by the solid line in Fig. 1. The fitting function is given as:

$$h(X)=h_{\rm sat}[1-\exp(-X/\tau)]\,, \tag{1}$$

where $h(X)$ is the Auger intensity at oxygen exposure $X=Pt$ (P is the O_2 pressure), $h_{\rm sat}$ is the Auger intensity after saturation oxidation, and τ is a constant. The good fit to Eq. (1), for the range of pressure used, shows that the adsorption rate depends linearly on the pressure for a given oxide coverage.

Based on the above results, an oxygen exposure of 2×10^7 L was used for "saturation" oxidation of the Sb in the rest of the experiments, except when noted otherwise.

B. AES for Sb deposits on Au(111)

Figure 2 is a plot of Au Auger intensity vs Sb coverage. Before oxidation, the decrease in the Au intensity with Sb coverage agrees well with earlier work.[9] Saturation oxidation causes little change in the Au Auger signal strength until after an Sb deposit of 1 ML, when the Au signal begins to drop below its value prior to oxygen exposure. There appears to be a break in the curve near 1.7 ML, with the Au signal reaching essentially zero by a Sb deposit of 2.5 ML.

Figure 3 shows the oxygen uptake for Sb films after saturation oxidation. The oxygen uptake is roughly proportional to the Sb coverage to about 0.9 ML, at which point there is a decrease in the slope of the uptake curve. The oxygen intensity is essentially constant after about 1.7 ML.

On deposition of the Sb, the Au Auger peak shifted 0.2 eV to lower energy, in agreement with earlier work.[9] After oxidation, the peak shifted back to the position for clean gold. This implies that the Sb-Au "bonds" are broken by the oxidation, and is consistent with the LEED observations below.

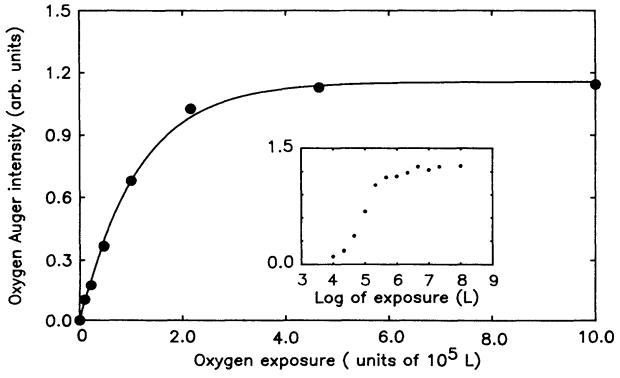

FIG. 1. Bulk Sb: oxygen Auger intensity as a function of oxygen exposure. (●), experimental; (–), theoretical fit. The inset is plotted as a function of the log of the exposure.

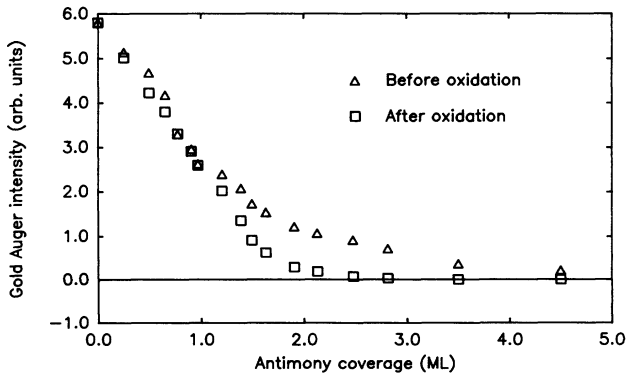

FIG. 2. Sb deposit: oxgyen Auger intensity as a function of Sb coverage, before and after saturation oxidation.

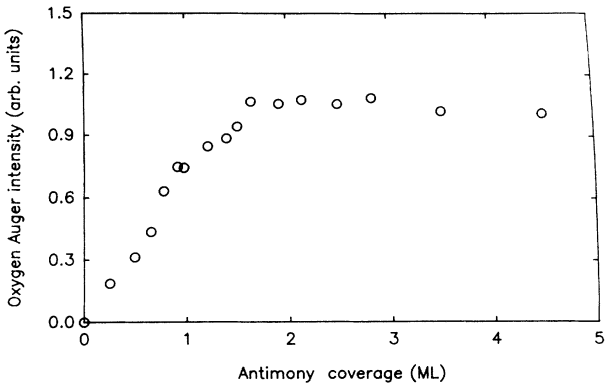

FIG. 3. Sb deposit: oxygen Auger intensity as a function of Sb coverage, for saturation oxidation.

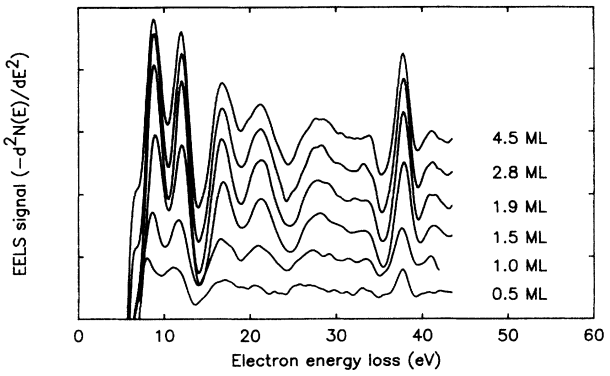

FIG. 5. Sb deposit: EELS signals for a range of Sb coverages, after saturation oxidation.

C. EELS

Figure 4 shows EEL spectra of the bulk Sb surface at various oxidation doses. Figure 5 presents the spectra of several Sb films after saturation oxidation. The main point to notice is that the top curves in these two figures are very similar, with the same peak positions and only minor differences in line shape.

D. LEED

For films thinner than 1 ML, a $(2\sqrt{3}\times 2\sqrt{3})R30°$ pattern was observed for pure Sb on Au(111), as seen previously.[9] No LEED pattern was observed for Sb oxide for either the films on Au(111) or the polycrystalline Sb surface. The $(2\sqrt{3}\times 2\sqrt{3})R30°$ pattern was totally gone after saturation oxidation for the smallest deposit observed, 0.25 ML. However, a faint Au(111) pattern could be seen for films thinner than 0.5 ML but disappeared for thicker films. These results indicate that the oxidation lifted the $(2\sqrt{3}\times 2\sqrt{3})R30°$ reconstruction of the first layer.

E. Work-function change

Only the work-function change of films on Au(111) was measured. The results are plotted in Fig. 6 for an oxygen exposure of 3×10^6 L. The work function increases slightly for Sb deposits up to 0.9 ML, and then decreases until the Sb coverage is about 1.8 ML. It remains constant for thicker films.

IV. DISCUSSION

A. Chemical composition

EELS can be used to identify the chemical composition of film oxides by comparison with the spectra of known bulk oxides, since it reflects the electronic and chemical environment in the surface. Table I compares the EELS peak positions for the oxide films and the oxide surface of bulk Sb with the result of Singh's work[11] on Sb_2O_3. The peak positions of the bulk Sb surface and film agree within the experimental uncertainty, while the EELS line shapes of the fully oxidized film and bulk surface are also similar (in Figs. 4 and 5). This shows that the chemical composition for the oxides on bulk Sb and on the Sb films is the same.

Comparing our EELS results with Singh's results, we see that the peak positions of Sb_2O_3 are systematically about 0.6 eV larger than those of the oxide produced in this experiment. This may be explained by the difference in work function of the analyzers used. The similarity of the peak positions between Sb_2O_3 and the oxide in our ex-

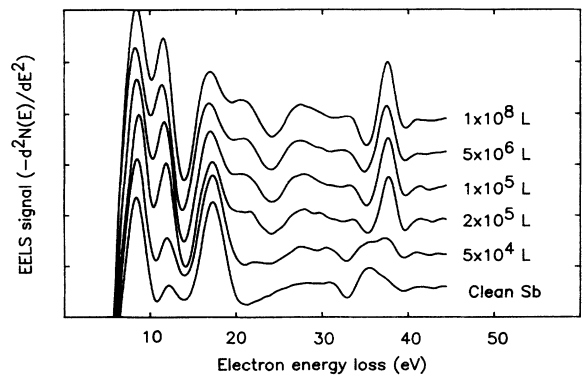

FIG. 4. Bulk Sb: EELS signals for a range of oxygen exposures.

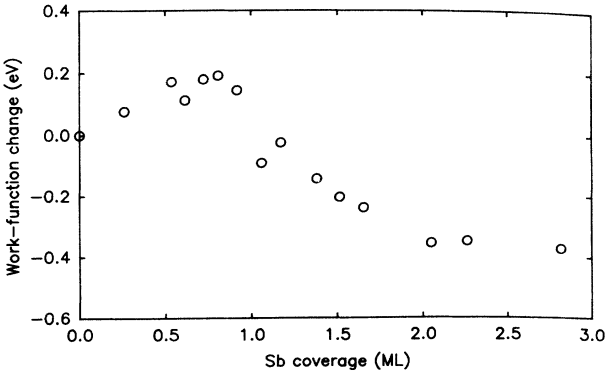

FIG. 6. Sb deposit: work-function change due to saturation oxidation, as a function of Sb coverage.

TABLE I. Comparison of EELS peak positions for Sb oxides.

	Peak positions (eV)							
This work								
Film on Au	8.7	11.5	16.8	21.3	28.0	33.8	37.7	41.2
Bulk	8.6	11.7	17.1	20.8	27.5	33.6	37.7	41.6
Sb_2O_3 (Ref. 11)	7.3	11.0	16.3	20.2	27.2	32.0	37.1	

periment shows that the latter is Sb_2O_3.

The loss peak for pure Sb at about 35 eV is due to the 4*d*-to-Fermi-level transition.[11] On saturation oxidation this peak undergoes a chemical shift of 2.3 eV to larger energy loss. This is very close to the value of 2.25 eV found by Petit, Riga, and Caudano[8] by x-ray photoemission spectroscopy (XPS) for the 3*d* level[8] for Sb_2O_3. Garbassi[12] found a core shift of 2.1 eV for oxidized Sb powder. However, Garbassi has also shown that the Sb peak positions in XPS for Sb_2O_3, Sb_2O_4 and Sb_2O_5 differ by only 1 eV in total, so that the core shift is not very useful in differentiating among the Sb oxides.

The bulk-plasmon energy for Sb_2O_3 can be calculated[13] to be 21.1 eV. The surface plasmon is then expected to have an energy of about 14.9 eV. These values are close to the positions of the peaks observed at 21.3 and 16.8 eV on the Sb film. Note that Singh[11] interpreted his peaks at 16.3 and 11.0 eV as being due to bulk- and surface-plasmon peaks of pure Sb, resulting from the dissociation of Sb_2O_3. However, as discussed above, dissociation should not be significant in our experiments. This conclusion is supported by the absence of the pure Sb peak near 35 eV after saturation oxidation in either Fig. 4 or 5. However, a rough calculation using electron attenuation lengths approximated by their inelastic mean free path (IMFP) values[14] shows that the bulk plasmon in the underlying Sb could contribute as much as 20% to the amplitude of the peak at 16.8 eV. We have been unable to locate a band structure for Sb_2O_3, and so cannot address the possible origins of the other peaks.

B. Auger line-shape decomposition

The kinetic energy of the Auger electrons from pure Sb is 457 eV, measured at the deepest lobe of the peak. The IMFP of these electrons in the oxide is about 14 Å,[14] while the thickness of the oxide layers produced in this experiment is about 8.5 Å, as shown below. Consequently, the oxide layer on bulk Sb is not thick enough to screen out the entire Auger signal from the underlying unoxidized Sb, even after saturation oxidation. Therefore, to extract more information about the oxidation from the Auger data, it is necessary to decompose the Sb signal into a pure Sb component and an oxide component. To do so, one has to know the line shapes of these components. Since the Auger line shapes of thick Sb films on Au(111) and of bulk Sb are identical, either can be chosen for the pure Sb component. The line shape of 1 ML of Sb on Au(111) after saturation oxidation has been chosen to represent the oxide line shape, because it has no component from unoxidized Sb, as shown below. The oxide component will be referred to as the SbO_x signal.

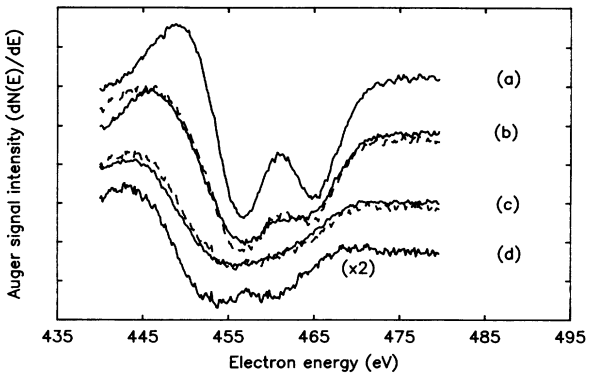

FIG. 7. Sb Auger line shapes. (a) Clean bulk Sb. After saturation oxidation: (b) bulk Sb, (c) 2.5-ML deposit of Sb, and (d) 1-ML deposit of Sb. (–), experimental; (— — —), fitted.

The coefficients of the pure Sb component and oxide component of an observed Auger line shape are calculated by least-squares fitting. Typical results for the decomposition are shown in Fig. 7. The fitting, for different film thicknesses and oxidation doses, is good overall. This supports conclusions that the same oxide is formed in the films and on the bulk and only one kind of Sb oxide occurs. We cannot be absolutely sure, of course, that the line shape for the 1-ML oxide is the same as for the oxide on the bulk metal. However, a number of facts support this assumption. (1) The use of the 1-ML oxide line shape gave a good fit to all of the composite oxide/metal line shapes. (2) The oxide line shape was the same for both 1- and 2-ML deposits on Au. (3) The EEL spectra were essentially identical for saturation oxidation of bulk Sb and of films of Sb-on-Au more than 2 ML thick, indicating that these oxides were chemically the same.

The Auger intensities of the Sb and SbO_x components for the bulk surfaces are plotted in Fig. 8, as a function of oxygen exposure. The SbO_x intensity is expressed as a multiple of the SbO_x intensity for 1 ML of Sb; the Sb intensity is given as a multiple of the intensity of the clean bulk Sb signal. The oxide signal becomes saturated at about 2×10^6 L, which is consistent with the oxygen uptake curve of Fig. 1. For the films (Fig. 9), the oxide sig-

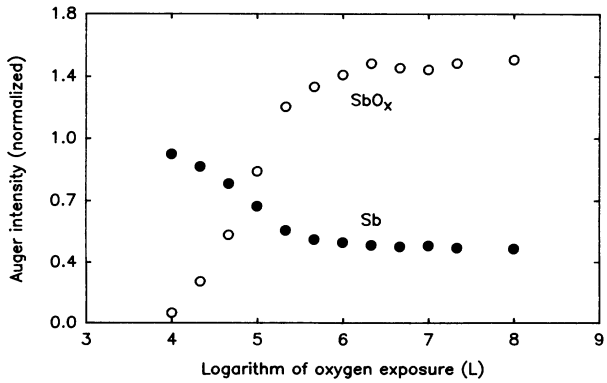

FIG. 8. Bulk Sb: Auger intensity of Sb and SbO_x as a function of $\log_{10}$ (oxygen exposure).

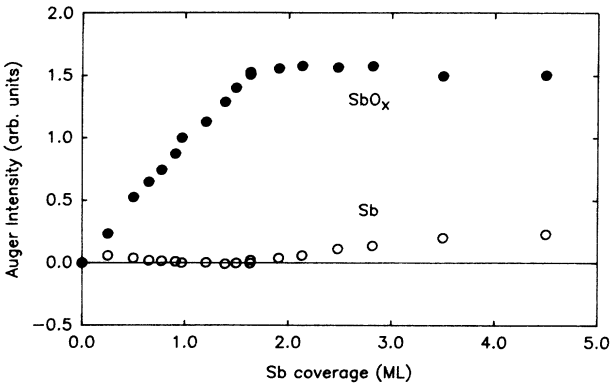

FIG. 9. Sb deposit: Auger intensity of Sb and SbO_x, for a range of Sb deposits on Au, after saturation oxidation.

nal increases in the region of Sb coverage less than 1.7 ML, while the pure Sb signals are essentially zero in this region. Above 1.7 ML, the oxide component remains constant and the pure Sb component begins to increase. This implies that films which are thinner than 1.7 ML are completely oxidized, while thicker films are not.

Figure 10 contains two plots: (1) the Auger amplitude of the Sb oxide vs that of oxygen for Sb films on Au(111) after saturation oxidation; and (2) the counterpart for the bulk surface, but at various oxygen doses. The data points for bulk Sb fall very close to a straight line; those for the Sb film show more scatter, which may be due to lack of reproducibility in the movement of the sample between the evaporator and the Auger analyzer for each datum point. The linearity of both plots shows that the stoichiometry of the oxide does not change as the film thickness changes. (By comparison, a similar plot for the oxide on Sn, which contains both SnO and SnO_2, did not appear linear at all.[6]) In addition, the two slopes differ by only 20%, which is not enough to indicate a difference in stoichiometry between bulk Sb and the film. Therefore, we conclude that only one kind of oxide formed at room temperature for both the Sb films on Au(111) and the bulk Sb surface. There is no obvious explanation for the slight differences in the slopes of these two plots.

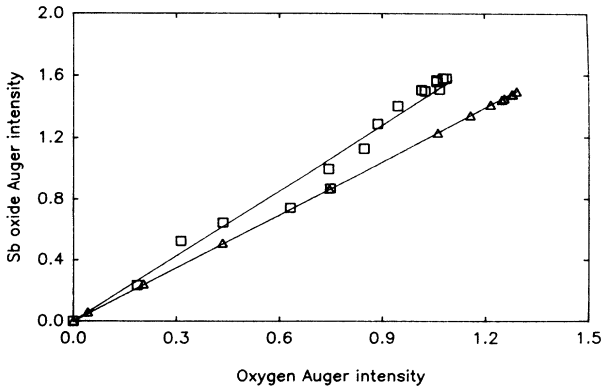

FIG. 10. SbO_x vs oxygen Auger intensities in arbitrary units. (△), for bulk Sb, for a range of oxygen exposures; and (□), for a range of Sb deposits on Au, after saturation oxidation.

Differences in the backscattering probability from the different substrates cannot be the only cause, because the maximum SbO_x intensity in Fig. 10 is slightly lower for bulk Sb, whereas the oxygen intensity is higher.

C. Thickness of the oxide layer

As discussed above, a complete oxide layer is formed for a deposit of 1.7 ML of Sb. The attenuation of the Au signal at this point can be used to calculate the thickness d of the oxide layer since

$$h_{\mathrm{Au}} = h^0_{\mathrm{Au}} \exp[-d/(0.75\lambda)] , \quad (2)$$

where h^0_{Au} and h_{Au} are the gold Auger intensities for the clean surface and after attenuation by the oxide layer, respectively. λ is the attenuation length of 69-eV electrons in Sb_2O_3, and the 0.75 accounts for the large collection angle of the analyzer used.[15,16] The attenuation length can be approximated by the theoretical value for the IMFP.[14] Using the energy gap for Sb_2O_3 of 4.20 eV,[17] the IMFP of 69-eV electrons in Sb_2O_3 is 5.4 Å, which from Eq. (2) yields $d = 8.5$ Å.

The thickness of the oxide layer on bulk Sb can be calculated in the same way. After saturation oxidation, the oxide layer has reduced the pure Sb signal to 45% of its value before deposition (see Fig. 8). The theoretical formula[14] yields an IMFP of 14.4 Å for the 457-eV electrons in Sb_2O_3. Substituting into Eq. (2) gives $d = 8.6$ Å, in excellent agreement with the earlier calculation. The absolute values of the theoretical IMFP (and hence the calculated values of d) may be larger than the values for the attenuation length by up to 35% because of elastic scattering.[18] However, this will not seriously alter the good agreement between values calculated above for the oxide thickness on bulk Sb and Sb films.

The density of Sb atoms in the oxide can be calculated from the knowledge that the density in one atomic layer is about $\frac{2}{3}$ of the Au density on the Au(111) surface;[9] i.e., 9.3×10^{14} Sb atoms/cm^2. Therefore, 1.7 ML of Sb will contain 1.6×10^{15} Sb atoms/cm^2. Since this much Sb forms an 8.5-Å-thick layer of oxide, the atomic density of Sb in the oxide will be 1.9×10^{22} cm^{-3}, although this value may be too small by up to 35% because of the approximation of the attenuation length by the IMFP. This agrees within the uncertainty in the IMFP with the Sb density of 2.31×10^{22} atoms/cm^3 for the bulk structure of cubic Sb_2O_3.[19]

D. Oxide growth mode

As discussed above, the thickness of the saturation oxide layer is about 8.5 Å both for bulk Sb and Sb films thicker than 1.7 ML. Since the final oxide layer incorporates almost two layers of Sb atoms, this raises the question of whether this oxide forms one layer at a time, or as a double layer. For the bulk sample, this oxide clearly grows laterally across the surface as a double layer, rather than layer by layer. This is shown by the fact that the oxygen uptake curve in Fig. 1 follows first-order Langmuir kinetics, which requires that the surface layer forms in a single step.

However, as found for Pb and Bi in earlier work,[4,5] we suggest that the oxide growth on the Sb film on Au(111) follows a two-step process: it develops as a monolayer until about 0.9 ML of Sb is deposited, and thereafter as a double layer of oxide in the region where the original Sb film is two atoms thick. The growth continues until the double layer is complete at a deposit of about 1.7 ML. The main evidence for this model comes from two sources. The first is the 0.5-ML EELS curve in Fig. 5. If the oxide were developing as a double layer, only about $0.5/1.7=0.29$ of the Au surface should be covered at this point. Therefore, one would expect to see significant loss peaks from both the Au bulk plasmon at 25 eV and the Au N_6-to-O_3 transition at 33 eV, yet neither has appreciable strength. The two-step oxidation process on the films is also seen in the oxygen uptake curve in Fig. 3. There is a clear decrease in slope for films thicker than about 0.9 ML of Sb, where the double layer of oxide begins to form, with no further uptake after a deposit of about 1.7 ML has been reached; i.e., at roughly twice the coverage needed to complete the first layer.

It also appears that, for a Sb deposit of less than 0.9 ML, the oxygen lies at least partly above the surface, whereas for thicker films the oxygen moves below the surface. The location of the oxygen is suggested by the work-function changes of Fig. 6: the work function increases until an Sb deposit of about 0.9 ML is reached, followed by a decrease until the oxide layer saturates near 1.8 ML. As the oxygen moves from outside the surface to inside, the surface dipole layer will change from negative outwards to positive outwards, producing this behavior.

We will now show that the other experimental results are consistent with this proposed growth model. If it is assumed that the decrease in slope after 0.9 ML in Fig. 3 is due solely to the formation of the second oxide layer, one can calculate the thickness of this second layer. This calculation gives about 8 Å, based on the Sb signal amplitudes for the 0.9-ML deposit and for the saturation oxide, and using the theoretical value for the IMFP calculated earlier. This is clearly much too large; the full thickness of the double layer has been calculated earlier to be only 8.5 Å. However, this rapid decrease in slope can be explained by the transfer of oxygen from above the surface to below it, as suggested by the work-function measurements.

The beginning of the double layer would also be expected to cause a break in the SbO_x curve in Fig. 9, as seen in the cases of Pb (Ref. 4) and Bi.[5] Indeed, a weak break is seen at 0.9 ML, where expected. That this break is not stronger can be explained again by the incorporation of oxygen below the surface; this would cause an apparent increase in the Sb AES signal over what would otherwise be expected, opposite to the effect seen for oxygen. The fact that this break is weaker than in corresponding plots for Pb and Bi is explained by the much shorter IMFP's for the Auger electrons used for Pb and Bi.

One would also expect that a two-step process would cause a noticeable break near 0.9 ML in the plot of Au Auger intensity vs Sb coverage after oxidation in Fig. 2 [and as seen for Bi (Ref. 5)], whereas this plot is quite linear in this region. However, this curve is anomalous in another way. The data for Sb deposits of less than about 1 ML show little reduction in the Au intensity from the oxidation, whereas beyond 1 ML this reduction is substantial. This increase in the attenuation of the Au signal after completion of the first oxide layer would tend to reduce the magnitude of the expected break near 0.9 ML, possibly enough to make the curve appear linear.

Some discussion is required of this absence of an attenuation of the Auger signal from the Au substrate, after adsorption of oxygen on the first deposit layer, since this effect was also seen for Pb (Ref. 3) and Bi.[5] The effect is surprising at first consideration, since the addition of electron density from the oxygen might be expected to reduce the IMFP of transmitted electrons. One possible explanation is that, for deposits of less than about 1 ML, the oxygen atoms adsorb on top of the surface in a chemisorbed state with the electrons in a localized bond. Therefore these electrons would not participate in the dominant loss processes of plasmon and electron-hole pair production which require an electron gas.[20] Only after the deposited layer is about two atoms thick can the oxygen move below the surface and an extended oxide be formed, with a decrease in the IMFP of the Auger electrons from the substrate. This hypothesis is supported by the behavior of the Sb_2O_3 surface-plasmon peak at 16.8 eV in Fig. 5, if we note that an Sb_2O_3 surface plasmon might be expected for less than a complete monolayer of oxide but not for a chemisorbed oxygen layer. For an Sb deposit of 0.5 ML, a peak near 16.8 eV is barely visible above the noise; at 1 ML it is just becoming significant, but by 1.9 ML it is fully developed.

However, the similarity in the Sb Auger line shapes for oxygen on top (chemisorbed) and underneath (surface oxide) remains a little surprising. Presumably this occurs because the atomic states involved in the $M_4N_{4,5}N_{4,5}$ transition in Sb are not valence states, and so are insensitive to the differences between a localized chemisorbed bond and a less localized bond in the extended oxide.

Finally, Fig. 1 shows that the initial sticking probability for oxygen on the Sb surface is about 10^{-5}, since 1 L is roughly the gas exposure required to deposit one monolayer of atoms on the surface when the sticking probability is unity.

V. CONCLUSIONS

It has been found that the adsorption of oxygen on bulk polycrystalline Sb follows first-order Langmuir kinetics at 300 K and for oxygen pressures in the range of 1×10^{-5}–2×10^{-3} Torr. The same initial oxide Sb_2O_3 forms on Sb films on Au(111) and on bulk Sb. At the completion of this initial fast-oxidation stage, the oxide layer is about 8.5 Å thick, and completely covers the surface for a Sb deposit of 1.7 ML. For Sb deposits less than about 0.9 ML thick, the oxide seems to grow initially with the oxygen on the surface; for Sb films thicker than 1.7 ML and for bulk Sb, the oxygen probably moves below the surface and the oxide develops as a "double layer" about 8.5 Å thick.

ACKNOWLEDGMENTS

Thanks are due to K. Fowler for technical support, and to E. Puckrin for many useful discussions. The generous donation of the gold crystal by Dr. M. Swanson (University of North Carolina) is much appreciated. Thanks are also due to NSERC, Canada, for financial support, and to CIDA, Canada, for support for P.M.

[1]F. P. Fehlner and N. F. Mott, Oxid. Met. **2**, 59 (1970).
[2]F. P. Fehlner, *Low-Temperature Oxidation* (Wiley, New York, 1986).
[3]J. G. Macmillan-Jones, F. A. Londry, and A. J. Slavin, Surf. Sci. **186**, 357 (1987).
[4]F. Peeters and A. J. Slavin, Surf. Sci. **214**, 85 (1989).
[5]E. Puckrin and A. J. Slavin, Phys. Rev. B **42**, 1168 (1990).
[6]Y. Zhang and A. J. Slavin, J. Vac. Sci. Technol. A **10**, 2371 (1992).
[7]A. J. Rosenberg, J. N. Butler, and A. A. Menna, Surf. Sci. **5**, 17 (1966).
[8]E. J. Petit, J. Riga, and R. Caudano, Surf. Sci. **251/252**, 529 (1991).
[9]P. Ma and A. J. Slavin, J. Vac. Sci. Technol. A **11**, 2003 (1993).
[10]G. Bachmann, J. Scholtes, and H. Oechsner, Mikrochim. Acta (Wien) **1**, 489 (1987).
[11]S. Singh, Ph.D. thesis, University of Keele, 1976.
[12]F. Garbassi, Surf. Interf. Anal. **2**, 165 (1980).
[13]S. Tanuma, C. J. Powell, and D. R. Penn, Surf. Interf. Anal. **11**, 577 (1988).
[14]S. Tanuma, C. J. Powell, and D. R. Penn, J. Vac. Sci. Technol. A **8**, 2213 (1990).
[15]M. P. Seah, Surf. Sci. **32**, 703 (1972).
[16]E. Puckrin and A. J. Slavin, J. Electron Spectrosc. Relat. Phenom. **57**, 202 (1991).
[17]*The Oxide Handbook*, 2nd ed., edited by G. V. Samsonov (IFI/Plenum, New York, 1982).
[18]A. Jablonski, Surf. Sci. **188**, 164 (1987).
[19]R. W. G. Wyckoff, *Crystal Structures*, 2nd ed. (Interscience, New York, 1982), Vol. 1.
[20]J. C. Ashley, C. J. Tung, and R. H. Ritchie, Surf. Sci. **81**, 409 (1979).